Manuscript for consideration as an article at eLife

Geomagnetic and visual cues guide seasonal migratory orientation in the nocturnal fall armyworm, the world's most invasive insect

Yi-Bo Ma[1, †], Gui-Jun Wan[1, †], Yi Ji[1], Hui Chen[1,2], Bo-Ya Gao[1], Dai-Hong Yu[3], Ai-Dong Chen[4], Eric J. Warrant[2], Yan Wu[5], Jason W. Chapman[1,6], Gao Hu[1,5 *]

1 State Key Laboratory of Agricultural and Forestry Biosecurity, College of Plant Protection, Nanjing Agricultural University, Nanjing 210095, China

2 Lund Vision Group, Department of Biology, Lund University, Sölvegatan 35, 22362 Lund, Sweden.

3 Plant Protection Station of Yuanjiang County, Yuanjiang 653399, China

4 Agricultural Environment and Resources Institute, Yunnan Academy of Agricultural Sciences, Kunming 650205, China.

5 Key Laboratory of Surveillance and Management of Invasive Alien Species, Guizhou Education Department, Department of Biology and Engineering of Environment, Guiyang University, Guiyang 550005, China.

6 Centre for Ecology and Conservation, University of Exeter, Penryn, Cornwall TR10 9FE, United Kingdom.

* *Correspondence to: Gao HU, 1 Weigang Road, Nanjing 210095, China. E-mail: hugao@njau.edu.cn*

† These authors have contributed equally to this work

Abstract

The navigational mechanisms employed by nocturnal insect migrants remain to be elucidated in most species. Nocturnal insect migrants are often considered to use the Earth's geomagnetic field for navigation, yet the underlying mechanisms of magnetoreception in insects remain elusive. We developed an indoor experimental system to investigate the integration of geomagnetic and visual cues in the seasonal orientation of a globally distributed pest moth, the fall armyworm (*Spodoptera frugiperda*), a highly invasive species which in the past decade has colonized almost all potentially habitable regions of the globe. Our results demonstrate that fall armyworms require both geomagnetic and visual cues for accurate migratory orientation, with visual cues being indispensable for magnetic orientation. When visual and geomagnetic cues are placed in conflict moths become disoriented, although not immediately, indicating that sensory recognition of the conflict requires time to process. We also show that the absence of visual cues leads to a significant loss of flight stability, which likely explains the disruption in orientation. Our findings highlight the essential and conserved role of visual cues in maintaining stable magnetic orientation in nocturnal migratory moths.

Introduction

Numerous species of larger nocturnal moths, particularly in the family Noctuidae (hereafter ‘noctuid moths’), undertake long-distance multigenerational migrations in the Northern Hemisphere. Every spring across North America and Eurasia, billions of noctuid moths move hundreds of kilometers northwards to summer breeding grounds in the temperate zone, and in the subsequent fall their progeny return to lower latitude wintering areas (Holland et al., 2006; Satterfield et al., 2020; Hu et al., 2016, 2025; Huang et al., 2024). These migrations take place almost exclusively high above the ground, where fast winds facilitate rapid windborne transport leading to population redistribution over long distances (Chapman et al., 2010, 2015; Hu et al., 2016; Huang et al., 2024). Some of the most abundant species involved in these migrations are the world’s most destructive agricultural pests, and thus they are of huge importance for food security and economic prosperity (Bauer & Hoye 2014; Satterfield et al., 2020; Guo et al., 2020; Hu et al., 2025). It is thus of paramount importance to understand all aspects of the migratory patterns of noctuid moths.

Tracking the seasonal progression of resources requires noctuid moths to move in

the appropriate direction (northwards in spring and southwards in fall), a process entailing three linked steps. Firstly, they determine the seasonally appropriate direction (north or south) in which to travel. Secondly, high-flying noctuid moths select transporting winds that are broadly aligned with this direction. Thirdly, they adopt self-powered flight headings which are more-or-less aligned with the wind but, when required, offset to some degree to correct for crosswind drift (Chapman et al., 2015; Hu et al., 2016). Each step requires use of one or more compass senses based on globally stable cues to determine the required direction and behavioral responses (Mouritsen, 2014).

However, migration at night poses a considerable navigational challenge for noctuid moths and other night-flying insects (Warrant et al., 2011; Mouritsen, 2014; Foster et al., 2018; Gao et al., 2024). This is because they cannot rely on the sun for compass information in the way that diurnally migrating butterflies and hoverflies do (Mouritsen et al., 2002; Srygley et al., 2008; Gao et al., 2020; Massy et al., 2021). Despite this challenge, radar, tagging, and tethered-flight studies demonstrate that many larger nocturnal moths are highly sophisticated navigators, capable of selecting and maintaining appropriate movement directions with a high degree of accuracy, even when flying high above the ground (Chapman et al., 2010; Dreyer et al., 2018ab; Menz et al., 2022; Chen et al., 2023; Dreyer et al., 2025). Their ability to achieve seasonally appropriate migration directions typically surpasses that of diurnal windborne insect migrants (Chapman et al., 2010; Hu et al., 2016; Werber et al., 2025), and even matches the capability of nocturnal songbird migrants (Alerstam et al., 2011, Chapman et al., 2016). Clearly, migratory noctuid moths must possess one or more accurate compass senses, but in all species bar one, the source of the compass information has yet to be elucidated (Warrant et al., 2011; Foster et al., 2018; Mouritsen, 2018; Freas et al., 2023).

The one exception to this lack of knowledge of the sensory basis of navigation in noctuid moths is the Bogong moth (*Agrotis infusa*) of Australia, which uses both a magnetic compass (Dreyer et al., 2018a) and a stellar compass (Dreyer et al., 2025) to migrate in seasonally appropriate directions. The Bogong moth is unique, however, among long-range migratory noctuids because a single generation makes bidirectional movements to and from a highly restricted geographic location in southeast Australia (Warrant et al., 2016), rather akin to the migration of eastern North American monarch butterflies to and from a restricted area of central Mexico (Reppert et al., 2016). This is distinct from most other noctuid moth migrants, whose multigenerational migrations involve back-and-forth movements between broad

latitudinal zones (Drake & Reynolds 2012; Chapman et al., 2015; Gao et al., 2020; Tong et al., 2022; Hu et al., 2025) rather than to precise locations. Thus other noctuid moths presumably do not require the same navigational precision, and may therefore be expected to have simpler sensory capabilities than the Bogong moth. We examine this question using the fall armyworm (*Spodoptera frugiperda*), one of the world's most serious crop pests, as a model for understanding general noctuid moth migration and navigation capabilities.

The fall armyworm is a migratory crop pest native to the Americas, where it breeds year-round in tropical regions and annually migrates into temperate regions of North America (Nagoshi & Meagher, 2008; Westbrook et al., 2019). Over the past 10 years, it has invaded and rapidly spread across Africa, Asia, and Australasia (Goergen et al., 2016; Kenis et al., 2023; Tay et al., 2023), assisted by its high migratory capacity (Chen et al., 2022, 2025; Gao et al., 2025), where it causes huge yield losses. Invasive fall armyworm populations now breed year-round in tropical regions of Southeast Asia and South China; each spring they migrate northwards as far as Northeast China, and the progeny resulting from summer breeding return southwards in the fall (Li et al., 2020; Sun et al., 2021; Wu et al., 2021; Wu et al., 2022). We recently found that fall armyworms from the year-round range in Southwest China (Yunnan) exhibit seasonally appropriate migratory headings when flown outdoors in virtual flight simulators, heading northward in the spring and southward in the fall, and this seasonal reversal is controlled by photoperiod (Chen et al., 2023). However, the compass mechanism that fall armyworms use to select seasonally appropriate headings remains unknown. The Earth's geomagnetic field is a ubiquitous and reliable source of compass information (Mouritsen, 2018), and thus might be expected to be the primary compass cue used by night-flying migratory moths. However, despite intriguing indications of magnetoreception in several species of migratory noctuids (Xu et al., 2017; Tong et al., 2022; Jin et al., 2023), so far only the highly specialised Bogong moth has been confirmed to use magnetic information for navigation (Dreyer et al., 2018a, Dreyer et al., 2025). To test whether more generalist noctuid moth migrants also rely on a magnetic compass for navigation, we investigated an invasive fall armyworm population in China using a newly developed tethered-flight assay designed to quantify migratory orientation. (Fig. 1). The results of these experiments are not only of fundamental interest to sensory biology, but are also of applied importance given that the fall armyworm is one of the most mobile and invasive crop pests in the world (Warrant & Dacke et al., 2011; Kenis et al., 2023; Tay et al., 2023).

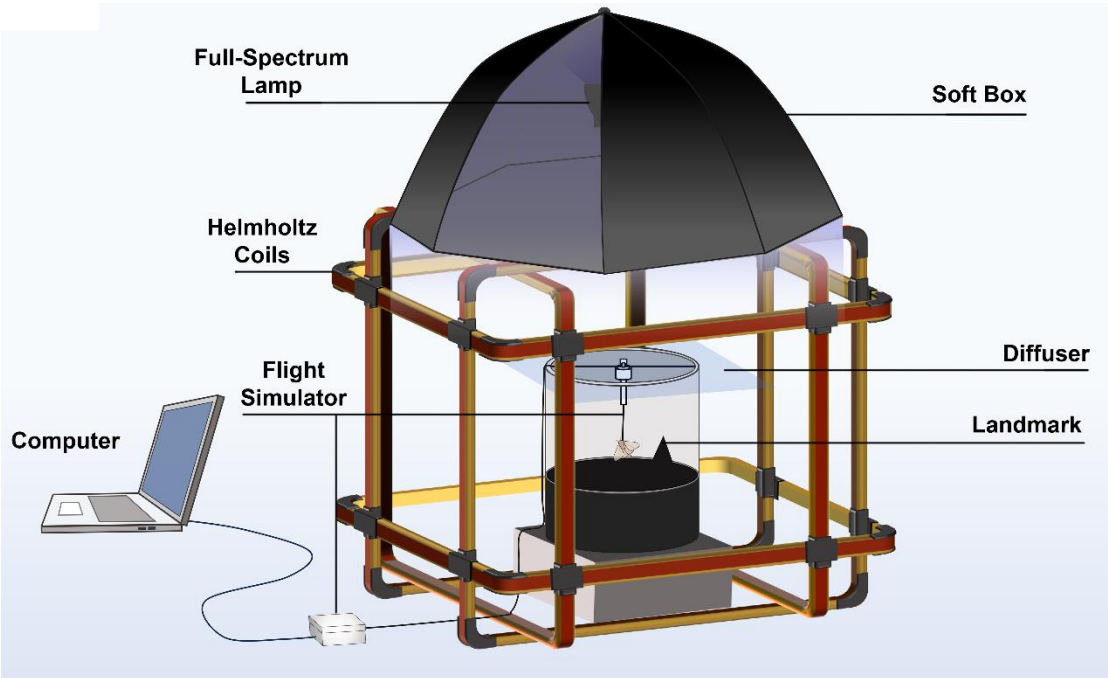

Fig. 1. Schematic of the experimental setup for studying magnetic orientation in fall armyworms. Moths are tethered to a vertical shaft at the center of the virtual flight simulator, with an encoder recording their flight heading. A full-spectrum lamp illuminates the arena, while the computer controlling the experiment is positioned outside the light field to avoid interference. Moths are free to rotate in any direction during the assay. Full experimental details in Methods. The cylinder is illustrated as clear in the figure to reveal the internal setup, but it is opaque in the actual experiment.

Results

Integration of geomagnetic and visual cues in the seasonal migratory orientation of fall armyworms

To examine if fall armyworms integrate geomagnetic and visual cues for seasonal migratory orientation, we measured flight responses of tethered moths within a virtual flight simulator (Dreyer et al., 2021) using a modified experimental approach used in Bogong moth studies (Dreyer et al., 2018a; Dreyer et al., 2025). The simulator consisted of a polyvinyl chloride (PVC) cylinder incorporating a visual cue on the side (a black triangle rising above a black horizon; Fig. 1). When tethered within the simulator, the moth is restrained but is free to rotate and thus take up any orientation it chooses. The simulator was placed within a 3D Helmholtz coil setup; under control conditions, the Earth's Natural Magnetic Field (NMF) was not affected, i.e., magnetic north and geographic north were closely aligned. However, when the coils were

switched on, they reversed the horizontal direction of the local magnetic field by 180° (the “Changed Magnetic Field”, CMF) relative to the NMF, while maintaining constant field intensity and inclination angle (Fig. S1). Thus the field direction within the experimental arena temporarily switches so that its “local magnetic north” is aligned with geomagnetic south (GMS) and its “local magnetic south” is aligned with geomagnetic north (GMN), but all other field parameters remain constant. The experimental setup consisted of recording moth flight headings across five consecutive 5-minute phases (I, II, III, IV, V) of tethered flight under different experimental conditions that involved changing the azimuthal alignment of the visual cue and the local horizontal magnetic field component with respect to GMN and GMS (Fig. 2, Fig. S1). In phases I and V moths were exposed to the NMF, whereas in phases II–IV moths were exposed to the CMF (Fig. 2). During spring migration trials, the visual cue was aligned with GMN (the expected migratory orientation in spring) at the start of the trial, whereas in fall migration trials the set-up was reversed, with the visual cue initially aligned with GMS (the expected migratory orientation in fall; Fig. 2).

The first two experiments involved field-captured moths tested during spring and fall migration periods (Figs. 2*A* and 2*B*). In phase I, the visual cue was aligned with the expected seasonal magnetic direction in the NMF, and as expected, moths exhibited significant group orientation towards the visual cue in both seasons (Spring: mean vector [MV] = 347.4°, vector strength [R^*] = 1.59, $P < 0.001$, Fig. 2*A-I*; Fall: MV = 183.6°, $R^* = 1.76$, $P < 0.001$; Fig. 2*B-I*). In phase II, the horizontal component of the geomagnetic field was rotated 180° (the CMF condition), creating a conflict between the visual cue direction and the expected magnetic orientation. Despite the shift in the magnetic field direction, moths continued to show significant group orientation toward the visual cue during this 5-minute period (Spring: MV = 319.1°, $R^* = 1.39$, $P < 0.005$, Fig. 2*A-II*; Fall: MV = 191.0°, $R^* = 1.16$, $P < 0.05$, Fig. 2*B-II*), indicating that, at least initially, the visual cue was dominant compared to the magnetic cue. During phase III, which was a second 5-minute period of the experimental conditions applied in phase II, moths lost their significant group-level orientation in both seasons (Spring: $R^* = 0.67$, $P > 0.05$, Fig. 2*A-III*; Fall: $R^* = 0.34$, $P > 0.05$; Fig. 2*B-III*), indicating that over time they had become confused due to the conflicting nature of the cues. The loss of group orientation was not due to fatigue or loss of directedness of individual moths, as flight vectors of individual moths had similar *r*-values in phases I–III (Figs. 2*A* and 2*B*; Table S2). In phase IV, the visual cue was realigned with the expected seasonal magnetic orientation, but this time in the CMF (i.e., the

192 cues were arranged in the same way as in phase I but rotated by 180°). Therefore,
193 the moths should not be able to distinguish between phase I and phase IV and thus
194 are expected to show the same orientation response in both phases. Indeed, the
195 moths tended to show group orientation towards the congruent cues once again,
196 albeit not quite reaching significance in spring (Spring: MV = 245.2°, $R^* = 0.95$, 0.05
197 $< P < 0.10$, Fig. 2*A-IV*; Fall: MV = 354.3°, $R^* = 1.49$, $P < 0.005$; Fig 2*B-IV*). Finally, in
198 phase V, the initial configuration was restored, and moths regained significant group
199 orientation toward the congruent visual cue and the expected magnetic orientation in
200 the NMF (Spring: MV = 343.8°, $R^* = 1.84$, $P < 0.001$, Fig. 2*A-V*; Fall: MV = 167.7°, R^*
201 $= 1.62$, $P < 0.001$, Fig 2*B-V*). These results demonstrate that fall armyworm
202 integrates geomagnetic field information with visual cues to achieve stable
203 orientation. However, when geomagnetic and visual cues do not align with expected
204 seasonal directions, moths gradually lose orientation, reinforcing the critical role of
205 cue integration in maintaining migratory stability.

206 Our previous research showed that fall armyworms reared under artificially simulated
207 fall conditions exhibited southward orientation in a flight simulator, consistent with the
208 behavior observed in wild individuals (Chen et al., 2023). To determine whether lab-
209 reared moths exposed to simulated seasonal photoperiods respond the same way to
210 geomagnetic and visual cues, we tested a population reared under a simulated fall
211 photoperiod in the same experimental setup as that of the field-captured fall group
212 (Fig. 2*C*). The results closely matched those from the field-captured wild population
213 (Fig. 2*B*). In phase I, with visual cues aligned to GMS in the NMF, lab-reared moths
214 oriented significantly southward (MV = 182.9°, $R^* = 1.77$, $P < 0.001$, Fig. 2*C-I*). When
215 the geomagnetic field was reversed (CMF), moths initially orientated towards the
216 visual cue, showing no immediate response to the shifted field (MV = 184.9°, R^*
217 $=1.31$, $P < 0.05$, Fig. 2*C-II*). After an additional 5-minute period without changes,
218 significant group-level orientation was lost ($R^* = 0.69$, $P > 0.05$, Fig. 2*C-III*). When the
219 visual cue was realigned with the changed GMS, significant orientation was restored
220 (MV = 4.1°, $R^* = 2.17$, $P < 0.001$, Fig. 2*C-IV*), though the direction was opposite that
221 in phase I. Finally, returning to the original setup restored the initial orientation pattern
222 (MV = 137.6°, $R^* = 1.04$, $P < 0.05$, Fig. 2*C-V*). These results demonstrate that lab-
223 raised fall armyworms integrate geomagnetic and visual cues similarly to wild
224 populations, emphasizing the role of photoperiod during development in shaping
225 seasonal multimodal migratory orientation.

226 To confirm that the loss of orientation in experimental groups was due to the cue
227 conflict rather than fatigue arising from a prolonged test duration, we conducted a

control experiment with the lab-raised simulated fall population, where the visual cue and GMS remained consistently aligned. In this group, moths maintained significant orientation in their expected migratory direction throughout the experiment when exposed to congruently-aligned cues, irrespective of whether under NMF or CMF conditions (Fig. 2*D*; directional statistics in Table S1). This confirms that the loss of orientation observed in experimental groups was driven by misalignment between visual and geomagnetic cues, rather than fatigue.

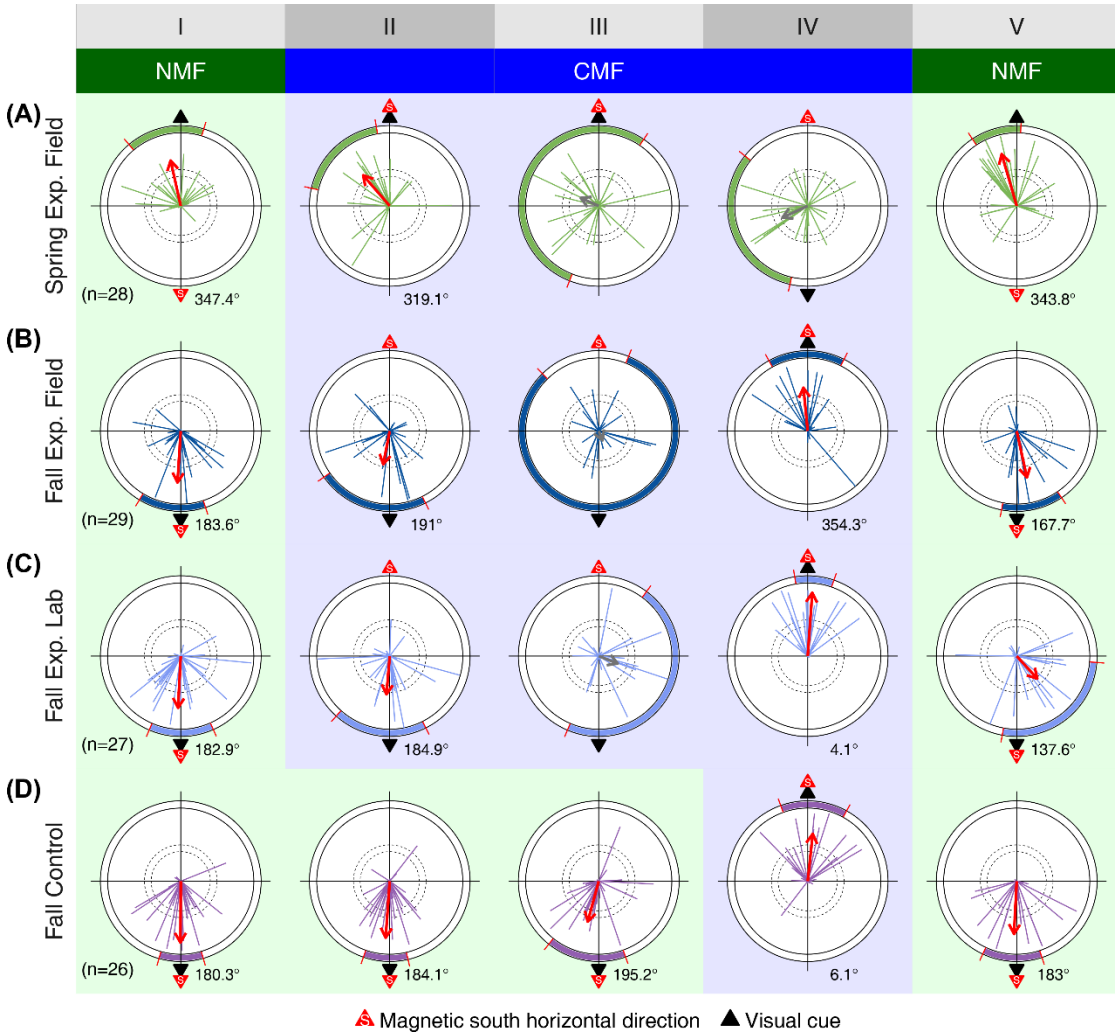

Fig. 2 The Earth's magnetic field and visual cues guide migratory flight behavior in both field-captured and lab-raised fall armyworms. (*A*) Flight orientation behavior of spring field-captured moths ("Spring Exp. Field") in response to visual and geomagnetic cues. (*B*) Flight orientation behavior of fall field-captured moths ("Fall Exp. Field") in response to visual and geomagnetic cues. (*C*) Flight orientation behavior of lab-raised fall-conditioned moths ("Fall Exp. Lab") in response to visual and geomagnetic cues. (*D*) Flight orientation behavior of lab-raised control fall-conditioned moths ("Fall Control"), tested with consistent visual and geomagnetic

alignment. Each group underwent five sequential 5-minute phases (I–V), with each subplot representing individual moths' flight directions in the simulator. The length of each vector represents individual directedness (*r*), ranging from 0 to 1, where the outer edge of the plot corresponds to $r = 1$. The thick mean vector (MV) arrow represents the weighted average of individual orientations, calculated using Moore's modified Rayleigh test (see Methods), and is red when there is significant group orientation but grey when it is not significant. The R^* value quantifies the directedness of the MV. Dashed circles indicate thresholds for statistical significance, with radii corresponding to $P < 0.05$ and $P < 0.01$. Shaded sections of the outer diameters of the circles represent the 95% confidence limits of the group orientation. The outermost radius represents $R^* = 2.5$. The black triangle denotes the position of the visual cue, while the red triangle indicates the direction of the expected migratory orientation in each season (north in spring, south in fall). The experimental setup included both the natural magnetic field (NMF, panels with light green background) and a changed magnetic field (CMF, panels with light blue background) where the horizontal magnetic field direction was reversed; further details of the magnetic field parameters in the NMF and CMF are shown in Fig. S1.

Fall armyworms show a delayed response to changes in magnetic fields

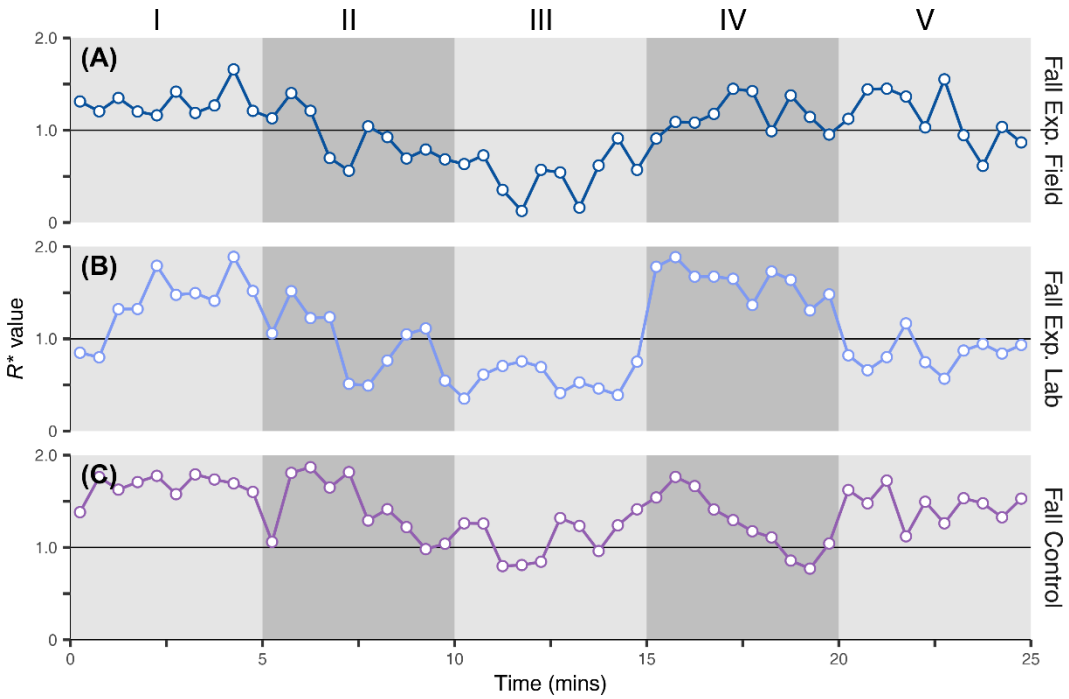

Fig. 3. Fall armyworms exhibit a delayed response to changes in magnetic-visual cue alignment. The behavioral data for (*A*) fall field-captured experimental ("Fall Exp. Field", data from Fig. 2B), (*B*) fall lab-raised experimental ("Fall Exp. Lab", data from Fig. 2C), and (*C*) fall lab-raised control ("Fall Control", data from Fig. 2D) groups were analyzed in 30-second time bins, resulting in ten bins over each 5-minute phase of the experiment. For each group,

Moore's modified Rayleigh test was applied, and the obtained R^* values were plotted against time. $R^* > 1$ indicates a significant collective orientation within that 30-second interval, while $R^* < 1$ indicates the absence of significant group-level orientation.

Our results show that migratory fall armyworms rely on both the Earth's magnetic field and visual cues to determine their flight direction. However, for moths to maintain constant orientation, the two sensory inputs must remain congruent, and when they come into conflict the moths become disoriented at the group level (but not at the individual level; Fig. 2). Notably, this response to the conflict between visual and geomagnetic cues was not instanteous but delayed until the second 5-minute experimental phase with this condition, consistent with similar results from Bogong moths (Dreyer et al., 2018a). Initial analyses using a 5-minute resolution provided limited temporal detail. To improve resolution, we subdivided each 5-minute phase into ten 30-second intervals and independently analyzed directional consistency using Moore's Rayleigh test to calculate the R^* for each 30-second period (Fig. 3).

During phase I, R^* values in both experimental groups remained >1 (Figs. 3*A-I* and 3*B-I*), indicating significant orientation behavior. When the magnetic field was rotated to conflict with visual cue directions, R^* values did not drop immediately but instead declined gradually over time (Figs. 3*A-II* and 3*B-II*). By phase III, R^* values were consistently <1, indicating a loss of significant orientation (Figs. 3 *A-III* and 3 *B-III*). Upon realigning the magnetic field with visual cues, R^* values showed a gradual increase, eventually exceeding 1 in both groups (Figs. 3*A-IV* and 3*B-IV*). When the original configuration was restored, the field-captured group consistently exhibited R^* values above 1 (Fig. 3*A-V*), while the lab-raised group had R^* values hovering around 1 (Fig. 3*B-V*). These results indicate that fall armyworms require time to resolve conflicting navigational inputs before losing group orientation entirely, or to react to congruent cues and regain group orientation. In the lab-raised control group, where the geomagnetic field and visual cues remained consistently aligned, R^* values consistently remained above 1 (Fig. 3*C*), confirming that the decline in group-level orientation observed in the experimental groups was driven by conflicts between geomagnetic and visual cues, mirroring the results found in Bogong moths (Dreyer et al., 2018a).

Visual cues are essential for magnetic orientation in fall armyworms

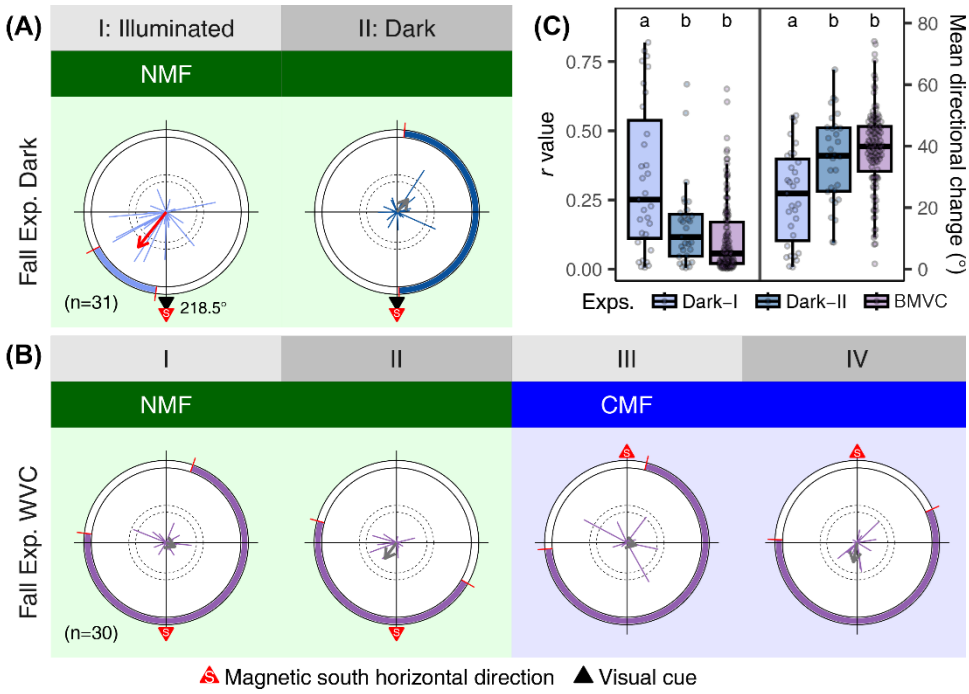

Fig. 4. Visual information is essential for maintaining group flight orientation in fall armyworms. (*A*) The lab-raised, fall-conditioned population lost significant group orientation under complete darkness ("Fall Exp. Dark"). (*B*) The lab-raised, fall-conditioned population exhibited a significant loss of group orientation under illuminated conditions where visual cues were reduced to the bare minimum ("Fall Exp. BMVC"), i.e., obvious visual cues such as the black triangle were not provided. (*C*) The distribution of Rayleigh test *r*-values for individual moth orientations across different treatment groups (*Left*), and the distribution of average directional change per second (*Right*), the latter reflecting flight stability. The box plots represent the interquartile range (IQR), with the horizontal line inside indicating the median. Whiskers extend to the most extreme data points within 1.5 times the IQR. Pairwise comparisons of the *r*-values were performed using the Mann-Whitney U test, with multiple comparisons corrected by the Benjamini-Hochberg method. Detailed statistical results are provided in Table S3. Comparisons of the average directional change per second were performed using one-way ANOVA followed by Tukey's HSD post hoc test, with statistical results provided in Table S4. Groups labeled with different letters differ significantly ($P < 0.05$). We also analyzed the *r*-values and average directional change per second in the Fall Exp. Field, Fall Exp. Lab, Exp. Fall Control, and the experiment shown in this figure, with results consistent with those shown here (see Tables S3 and S4, Fig. S4).

Growing evidence supports the idea that geomagnetic cues provide essential compass information for orientation across a broad range of taxa, supporting diverse navigational tasks (Mouritsen, 2018; Dreyer et al.,2018a; Fleischmann et al., 2018; Wan et al., 2021; Xu et al., 2021; Grob et al., 2024; Goforth et al., 2025). To determine whether geomagnetic input alone is sufficient for flight orientation in fall armyworms, we conducted a series of experiments to evaluate the role of visual cues in their orientation behavior. In particular, we examined whether these moths could maintain orientation in the absence of visual cues.

As a control, we first tested lab-raised, fall-conditioned moths in an arena where visual landmarks were aligned with GMS in the NMF (Fig. 4*A*). When illuminated, moths showed significant group orientation towards the visual cue (MV = 218.48°, R^* = 1.50, $P < 0.005$, Fig. 4*A-I*), consistent with our previous results (Fig. 2*B*). To determine whether moths could maintain orientation without visual information, we then removed all light sources, allowing moths to continue flying in total darkness. Under these conditions, moths lost significant group-level orientation (R^* = 0.5, $P > 0.05$, Fig. 4*A-II*), suggesting that their orientation behavior is dependent on the presence of light. The loss of orientation may be due to the absence of usable visual landmarks, or the lack of light in a dark environment causing the moths to lose their sense of direction. However, it is still unclear how the absence of usable visual landmarks in non-dark environments would affect the moths' orientation behavior.

To further investigate this, we tested a lab-raised, fall-conditioned population of moths in a simulator, primarily to determine whether moths could maintain orientation under illuminated conditions where visual cues on the interior walls of the cylindrical flight arena were minimized. In this experiment, we provided a uniform visual environment (i.e., under illuminated conditions, visual cues were not provided on the interior walls of the cylindrical flight arena). After recording 10 minutes of orientation behavior under the NMF, we reversed the horizontal component of the geomagnetic field using Helmholtz coils (CMF) and recorded their flight orientation for an additional 10 minutes. Despite the altered magnetic field direction and sufficient time for adaptation, moths exhibited no significant group orientation across all four testing phases (Fig. 4*B*; directional statistics in Table S1). The lack of group-level orientation under near-uniform visual conditions suggests two possibilities: individual moths may have maintained stable flight, but due to the absence of reliable orientation cues, their group-level directional choices were random; or their flight may have been unstable, making it difficult to assess individual orientation behavior. We first compared the differences in the Rayleigh test *r*-values of moths across different

experimental phases (Fig. 4*C*, *Left*), using the Wilcoxon rank-sum test and applying the Benjamini-Hochberg procedure to control for false positives in multiple comparisons. This is because the Rayleigh test evaluates the concentration of data, with an *r*-value close to 1 indicating highly consistent flight directions, and close to 0 suggesting more random flight directions. The results showed that under conditions with visual cues (Fall Exp. Dark-I), moths had significantly higher *r*-values compared to conditions of complete darkness (Fall Exp. Dark-II) or visual cues reduced to the bare minimum (Fall Exp. BMVC).

We also considered the limitations of the Rayleigh test, as its *r*-value only reflects the overall directional tendency and does not reveal real-time flight stability. For example, a moth exhibiting two stable flight phases, one oriented north and the other south, would yield a low *r*-value despite maintaining stability within each phase. Conversely, a moth losing flight stability could also produce a low *r*-value, making it difficult to distinguish between these two scenarios based on *r*-value alone. Therefore, we introduced the analysis of per-second angular change (Fig. 4*C*, *Right*) to assess dynamic fluctuations in flight behavior, providing a clearer understanding of whether the observed differences in *r*-values were due to stable orientation or a loss of flight control. Our analysis revealed that flight stability did not significantly differ among experimental groups, except for those tested in conditions lacking visual cues (Fig. 4*C*, *Right*; Fall Exp. Dark-II & Fall Exp. BMVC). Moths in these conditions exhibited significantly higher angular change rates, indicating a greater tendency to alter flight direction and an inability to maintain stable orientation. Notably, even though a small subset of individuals in these groups managed to sustain stable flight, their directional choices appeared random rather than goal-oriented (Figs. 4*A-II* and 4*B*).

Discussion

The integration of geomagnetic and visual cues for flight orientation has so far been experimentally demonstrated only in the Australian Bogong moth, a species undertaking a precisely oriented, long-distance round-trip migration to and from a highly restricted aestivation site within a single generation (Dreyer et al., 2018a). Although this life-history strategy is uncommon among migratory insects, our development of an indoor behavioral paradigm in the fall armyworm, a globally distributed nocturnal migratory insect with multi-generational and partially migratory patterns in China, extends this dual-cue orientation strategy to a species exhibiting a migratory ecology more typical of insects in general. These findings demonstrate that this navigational mechanism is not unique to the Bogong moth and may instead

represent a conserved orientation mechanism broadly employed across migratory moth species. Crucially, we show that visual cues are indispensable for magnetic orientation in the fall armyworm, as directional responses disappeared in the absence of structured visual input. Furthermore, our findings reinforce recent results on seasonal shifts in orientation behavior in this species (Chen et al., 2023), highlighting the ecological relevance of this guidance system.

Our findings thus emphasize the importance of integrating multiple cues for successful navigation. It is often assumed that animals lack magnetic orientation capabilities if they fail to orient under changes in the geomagnetic field, either in appropriate lighting conditions or in darkness, without additional cues. However, our study demonstrates that the absence of group seasonal orientation under geomagnetic fields, in full-spectrum light or in darkness, does not preclude magnetic orientation when additional sensory cues are integrated. Specifically, a magnetic compass provides global directional cues for fall armyworms, enabling them to align magnetic north (or magnetic pole) and south (or magnetic equator) with visual cues during spring and fall, respectively, to facilitate seasonal orientation—a hallmark of annual long-distance migration in migratory species. Although the magnetic compass is critical, as evidenced by the loss of group orientation when the horizontal geomagnetic field was reversed while intensity and inclination remained unchanged, our results reveal that magnetic orientation cannot occur without appropriate visual cues. We also show that the loss of flight stability observed when visual cues are minimal is likely a major cause of the lack of group magnetic orientation. This highlights the complexity of magnetic orientation strategies in nocturnal migratory insects, emphasizing the crucial interaction between the magnetic compass and visual navigation systems. Further investigation by altering the geomagnetic polarity and vertical geomagnetic component is required to determine whether the magnetic compass guiding seasonal orientation in nocturnal migratory fall armyworms is polarity-sensitive, inclination-sensitive or both, which is pivotal to understanding the biophysical mechanisms underlying magnetoreception (Mouritsen, 2018; Hore et al., 2016; Grob et al., 2024).

Desert ants and Bogong moths have also been shown to integrate geomagnetic and visual cues for navigation. Desert ants rely on a magnetic compass during look-back-to-the-nest behavior, combining magnetic cues with local visual landmarks, such as their nest (Grob et al., 2024). In contrast, Bogong moths have been demonstrated to integrate global stellar cues with the Earth's magnetic field for long-distance navigation (Dreyer et al., 2025). Like Bogong moths, fall armyworms can migrate

hundreds, or even thousands, of kilometers over several successive nights (Warrant et al., 2016; Li et al., 2020). Global stellar cues or transient local landmarks encountered en route may contribute to geomagnetic-visual navigation in fall armyworms. However, whether their multimodal orientation strategy relies primarily on local visual cues, global visual cues, or an integration of both, remains to be elucidated. Future research will also be pivotal in further exploring the genetic and ecological underpinnings of multimodal navigation in migratory species.

In conclusion, our findings underscore the indispensability of visual cues in facilitating seasonal magnetic orientation, highlighting the complex, multimodal nature of navigation in nocturnal migratory insects. This work advances our understanding of migratory navigation strategies, suggesting the conservation of these mechanisms across long-distance migratory moths. Furthermore, the application of genome editing in fall armyworms, combined with the indoor behavioral paradigm developed here, provides a promising avenue for dissecting the molecular basis of magnetoreception and the interplay between sensory systems.

Methods

Field population

All wild populations used in this study were collected from farmland in Yuanjiang Hani and Yi Autonomous County, Yunnan Province, a region primarily characterized by maize cultivation. Fall-generation populations were collected during September to October of 2023 and 2024, while spring-generation populations were collected from April to May in 2024, as mature larvae at the 5th to 6th instar stages. Each larva was individually collected and reared in a cylindrical container, fed with fresh maize leaves from the collection site until pupation. Upon pupation, larvae were transferred to transparent, thin plastic cups sealed with plastic film. A cotton ball moistened with water was placed in each cup to maintain adequate humidity during the pupal stage. After eclosion, adults were individually provided with a 10% honey solution. All experimental individuals were reared at the Yuanjiang Plant Protection Station, a facility located near agricultural fields and well isolated from urban light pollution. To maintain natural environmental conditions, all electrical devices were strictly excluded from the facility, and windows were kept open around the clock to allow for natural light cycles and ambient temperature conditions.

466

467 **Lab-raised population**

468 The laboratory-reared population of the fall armyworm used in this study was
469 primarily derived from wild individuals collected from a maize field in Yuanjiang,
470 Yunnan Province (Google Maps coordinates: 23.604°N, 101.977°E) during October
471 to November 2022, with the exception of individuals used in experiments Fall Exp.
472 Dark and Fall Exp. BMVC (see Fig. 4), which were collected from the same field
473 location during October to November 2024. All experiments were conducted using
474 individuals from the 3rd to 5th laboratory-reared generations.

475 For behavioral assays conducted under ambient temperature conditions, a
476 programmed photoperiodic regimen was implemented to simulate the seasonal
477 changes in day length typical of autumn in East Asia. All treatments were maintained
478 at a constant temperature of 27 ± 1°C and a relative humidity of 60% ± 5%. In the fall
479 photoperiod treatment, the initial light cycle at egg hatching was set to 13 hours of
480 light and 11 hours of darkness (13L:11D), followed by a daily reduction of 2 minutes
481 in the light period. By the time adult moths emerged and were subjected to
482 experimental testing approximately one month later, the photoperiod had been
483 adjusted to approximately 12L:12D.

484 **Attachment of tethering stalks on moths**

485 We used the same method for the attachment of tethering stalks on moths as in the
486 previous study on fall armyworm moth orientation (Chen et al. 2023). Prior to
487 tethering, 2-day-old moths were housed in plastic cups and sedated at 4°C for at
488 least 1 minute to facilitate handling. The moths were then transferred to an
489 operational platform, where scales were carefully removed from the junction of the
490 dorsal thorax and abdomen to ensure secure attachment. The tether consisted of a
491 slender, non-magnetic copper stalk measuring 0.75 mm in diameter and
492 approximately 2 cm in length. The terminal end of the stalk was bent into a fork-like
493 structure, which was carefully affixed to the prepared thoracic-abdominal junction
494 using Pattex PSK12CT-2 glue. To maintain consistency, this standardized tethering
495 method was applied uniformly across all experimental protocols.

496 **Behavioral apparatus**

497 Our flight simulator system (Dreyer et al., 2021) is consistent with the one used in

previous research on FAW (Chen et al., 2023), utilizing the Flash flight simulator system. This system, developed by Hui Chen, is an improvement on the early design of the Mouritsen-Frost flight simulator, and is designed to support our experiments conducted in Yuanjiang (longitude 101.98°E, latitude 23.60°N). The moths are able to freely rotate on the horizontal plane within the simulator, with their azimuth measured by an encoder system with a resolution of 0.9°. The flight direction (relative to magnetic north) is recorded in real time by the Flash flight simulator data acquisition system developed by Hui Chen, and the data is saved as angle values in a text file. In our experiments, the encoder (made of non-magnetic materials) samples the azimuth five times per second and is equipped with a graphical interface, which allows for continuous monitoring of the moth's azimuth and flight status to reconstruct the flight path. The encoder is connected to the axis that holds the moth, with the axis measuring 15 cm in length and 1 mm in diameter, made of carbon fiber material and wrapped in a carbon fiber tube to protect its structure.

The arena consists of an opaque PVC cylinder with a diameter of 400 mm, a height of 500 mm, and a thickness of 5 mm as the main structure, surrounded by white wallpaper, with a 20 cm high black wallpaper strip at the bottom simulating the horizon. A visual cue is provided by a black isosceles triangle (10 cm high, 10 cm base) made from black wallpaper and fixed to the horizon at the bottom of the arena. The entire arena is placed on a square wooden board with a side length of 50 cm and a thickness of 1 cm, covered with black blackout cloth. The bottom of the wooden board is equipped with a plastic base to reduce friction, ensuring that the arena can rotate smoothly and quickly during the experiment, changing the direction of the visual cues while avoiding interference with the moth's activity.

In the BMVC experiment, we used an opaque white acrylic cylinder with the same dimensions as the PVC cylinder as the arena. No modifications were made to the interior of the arena, primarily because the interior of the white acrylic cylinder is smooth and uniform enough, and any additional treatment could potentially introduce noticeable visual cues. We also removed the carbon fiber crossbar used to fix the simulator and instead fixed it directly to the top acrylic cover to further minimize potential visual cues that the moth might use. Our goal was to minimize the visual cues available to the moth as much as possible, rather than attempting to completely eliminate all visual cues.

The experiment uses a full-spectrum light, which is enclosed in a 90 cm diameter GODOX softbox to ensure even distribution of light within the experimental arena.

The softbox is fixed to a Helmholtz coil, with the flight simulator located at its center. The top of the arena is equipped with a UV-transmitting acrylic panel and covered with Lee Filters 250 semi-white diffusion paper to control the amount of light transmitted. Spectral measurements are taken using a spectrometer to ensure consistency across trials (see Fig. S3). The spectral distribution of the full-spectrum light used in the experiment was measured using an ATP2000P spectrometer (Xiamen Spectral Technology Co., Ltd.).

Artificial simulation of the Earth's magnetic field

A three-dimensional pair of Helmholtz coils (Nanjing Science Sky Technology Limited) was used to manipulate the Earth's magnetic field. The coils measured 1200 × 1100 × 1000 mm, with a cold-state direct current resistance of 2Ω per coil and an insulation resistance exceeding 10MΩ. The magnetic field strength at the central X, Y, and Z axes exceeded 10 GS@6A (maximum current), with a spatial uniformity of 0.5% within a φ144 × 144 × 144 mm volume. At the start of each experiment, we used a TM4300B handheld three-axis fluxgate magnetometer to measure the ambient magnetic field strength and spatial vector intensity at the experimental site (averaged over three measurements). A programmable power supply with adjustable current and voltage was employed to apply a controlled current to the 3D Helmholtz coils, reversing the horizontal geomagnetic component by approximately 180°. Crucially, we ensured that total magnetic field intensity (E), horizontal component intensity (H), and magnetic inclination angle (α) remained statistically unchanged between the controlled magnetic field (CMF) and the normal magnetic field (NMF) (see Fig. S1).

Experimental procedure

The orientation experiment followed the protocols established in our previous study (Chen et al. 2023). Experiments began after complete darkness in the night sky: the field population were tested after adapting to the natural dark environment for at least 60 minutes, while the lab-reared population started after adapting to the dark environment for at least 60 minutes following the light-to-dark cycle switch in the incubator, in a laboratory away from large electrical equipment, artificial noise, plants, and other potential sources of interference. The computer screen was positioned away from and facing away from the experimental setup. Weak red light was used

565 only when attaching the tethering stalks and fixing the moth to the simulator. After the
566 moth was fixed, a waiting period of 20 to 30 seconds was allowed for the subject to
567 stabilize before data recording began. During this process, it was verified whether the
568 insect could switch between clockwise and counterclockwise rotations. If the insect
569 rotated in only one direction and could not fly stably, no further experiment was
570 conducted. The encoder's horizontal placement was also checked to ensure it was
571 not affected by tilting. The moth's wing vibrations were confirmed to be strong, with
572 equal amplitude on both wings (indicating that the contact glue did not interfere with
573 the wings). During the experiment, the insect's flight state was monitored by
574 observing fluctuations in the pointer values on the experimental software. If the
575 values did not change within 10 seconds, the experimenter needed to approach the
576 flight arena and listen for any sounds of wing vibrations. If the insect stopped flying,
577 the experimenter gently tapped the wall to stimulate the insect to continue flying. We
578 analyzed individuals that were able to maintain fewer than four instances of
579 wingbeats cessation during the experiment.

580 **Statistical analysis**

581 All statistical analyses and graph generation were performed using R (version 4.1.3),
582 accessible at https://www.r-project.org/. A custom R script, incorporating bootstrap
583 confidence intervals, was used for Moore's Modified Rayleigh Test (MMRT)—a non-
584 parametric test increasingly applied in orientation behavior studies. MMRT accounts
585 for both mean directions and directedness (vector lengths) of individuals, making it
586 an alternative to the Rayleigh test. MMRT assesses whether a group exhibits
587 significant directional tendencies, using the parameter R^* (a scaled alternative to r in
588 circular regression), which quantifies the strength of orientation within a group, and
589 the mean vector (MV), which represents the rank-weighted mean direction of the
590 group. Polar plots display individual vectors, with each vector representing an
591 individual moth's mean flight direction and directedness (r-value). The vector length
592 reflects the proportion of time a moth maintains a particular direction, ranging from r
593 = 0 (completely un-oriented) to r = 1 (fully oriented). MMRT requires the analysis of
594 each individual's average direction and r-value to determine the group-level mean
595 MV. It is important to note that the magnitude of R^* is dependent on sample size. To
596 assess the directional orientation of moths in different treatment groups, we
597 performed Rayleigh tests on individual flight directions to determine whether each
598 moth exhibited significant unimodal orientation. The resulting Rayleigh r-values for
599 each individual were used to compare orientation strength across treatment groups.
600 Pairwise comparisons were conducted using the Mann-Whitney U test, with multiple

comparisons corrected using the Benjamini-Hochberg procedure to control the false discovery rate (FDR). Detailed statistical results are provided in Table S3.

To assess flight stability, we calculated the average directional change per second by measuring the angular difference between successive seconds of recorded flight behavior. This metric reflects the consistency and stability of individual flight orientation. Differences among treatment groups were assessed using one-way ANOVA, followed by Tukey's Honest Significant Difference (HSD) post hoc test for pairwise comparisons. Groups labeled with different letters differ significantly ($P < 0.05$). Detailed statistical results are provided in Table S4.

Acknowledgements

This work was supported by the National Key Research and Development Program of China (2021YFD1400700) and the Fundamental Research Funds for the Central Universities (KJJQ2025013) to G.H., and the National Natural Science Foundation of China to (32202289) B.Y.G.

References

Alerstam T, Chapman JW, Bäckman J, Smith AD, Karlsson H, Nilsson C, Reynolds DR, Klaassen RHG, Hill JK, 2011. Convergent patterns of long-distance nocturnal migration in noctuid moths and passerine birds. *Proc. R. Soc. B* **278**:3074-3080. DOI: https://doi.org/10.1098/rspb.2011.0058

Bauer S & Hoye BJ, 2014. Migratory animals couple biodiversity and ecosystem functioning worldwide. *Science* **344**:54-62. DOI: https://doi.org/10.1126/science.1242552

Chapman JW, Nesbit RL, Burgin LE, Reynolds DR., Smith AD, Middleton DR, Hill JK. 2010. Flight orientation behaviors promote optimal migration trajectories in high-flying insects. *Science* **327**:682-685. DOI: https://doi.org/10.1126/science.1182990

Chapman JW, Reynolds DR, Wilson K, 2015. Long-range seasonal migration in insects: mechanisms, evolutionary drivers and ecological consequences. *Ecol. Lett.* **18**:287-302. DOI: https://doi.org/10.1111/ele.12407

Chapman JW, Nilsson C, Lim KS, Bäckman J, Reynolds DR, Alerstam T, 2016. Adaptive strategies in nocturnally migrating insects and songbirds: contrasting responses to wind. *J. Anim. Ecol.* **85**:115-124. DOI: https://doi.org/10.1111/1365-2656.12420

Chen H, Wang Y, Huang L, Xu CF, Li JH, Wang FY, Cheng W, Gao BY, Chapman JW, G. Hu, Flight capability and the low temperature threshold of a Chinese field population of the fall armyworm *Spodoptera frugiperda*. *Insects* **13**:422 (2022). DOI: https://doi.org/10.3390/insects13050422

640 Chen H, Wan GJ, Li JC, Ma YB, Reynolds DR, Dreyer D, Warrant EJ, Chapman JW,
641 G. Hu, Adaptive migratory orientation of an invasive pest on a new continent.
642 *iScience* **26**:108281 (2023). DOI: https://doi.org/10.1016/j.isci.2023.1082 81

643 Chen H, Xu CF, Wang YH, Li XR, Yu DH, Chen AD, Lyu BQ, Wu YF, Wang YM,
644 Chapman JW, G. Hu, Characteristics and seasonal variation of fall armyworm
645 migratory behavior in their year-round breeding areas in South China. *Pest*
646 *Manag. Sci.* **81**:4051-4062 (2025). DOI: https://doi.org/10.1002/ps.8772

647 Drake VA & Reynolds DR. 2012. Radar entomology: observing insect flight and
648 migration. Wallingford, UK: CABI

649 Dreyer D, Frost B, Mouritsen H, Günther A, Green K, Whitehouse M, Johnsen S,
650 Heinze S, Warrant E, 2018a. The Earth's magnetic field and visual landmarks
651 steer migratory flight behavior in the nocturnal Australian Bogong moth. *Curr.*
652 *Biol.* **28**:2160-2166. DOI: https://doi.org/10.1016/j.cub.2018.05.030

653 Dreyer D, el Jundi B, Kishkinev D, Suchentrunk C, Campostrini L, Frost BJ,
654 Zechmeister T, Warrant EJ, 2018b. Evidence for a southward autumn migration
655 of nocturnal noctuid moths in central Europe. *J. Exp. Biol*. **221**:jeb179218. DOI:
656 https://doi.org/10.1242/jeb.179218

657 Dreyer D, Frost B, Mouritsen H, Lefèvre A, Menz M, Warrant EJ, 2021. A guide for
658 using flight simulators to study the sensory basis of long-distance migration in
659 insects. *Front. Behav. Neurosci.* **15**:678936. DOI: https://doi.org/10.3389/fnbeh.
660 2021.678936

661 Dreyer D, Adden A, Chen H, Frost B, H. Mouritsen, J. J. Xu, K. Green, M.
662 Whitehouse, J. Chahl, J. Wallace, G. Hu, J. Foster, S. Heinze, E. J. Warrant,
663 2025. Bogong moths use a stellar compass for long-distance navigation at night.
664 *Nature* **643**:994-1000. https://doi.org/10.1038/s41586-025-09135-3

665 Fleischmann PN, Grob R, Müller VL, Wehner R, Rössler W, 2018. The geomagnetic
666 field is a compass cue in *Cataglyphis* ant navigation. *Curr. Biol*. **28**:1440-1444.
667 DOI: https://doi.org/10.1016/j.cub.2018.03.043

668 Freas CA & Spetch ML, 2023. Varieties of visual navigation in insects. *Anim. Cogn.*
669 **26**:319-342. https://doi.org/10.1016/j.conb.2011.05.020

670 Foster JJ, Smolka J, Nilsson DE, Dacke M, 2018. How animals follow the stars. *Proc.*
671 *R. Soc. B* **285**:20172322. DOI: https://doi.org/10.1098/rspb.2017.2322

672 Fu P, Li X, Sun Z, Chen Y, Lu Z, Tian C, Hu G, Gui F, 2025. Population genetics and
673 trajectory simulation reveals the invasion process of the fall armyworm
674 (*Spodoptera frugiperda*) in the Eastern Hemisphere. *Evol. Appl.* **18**:e70086. DOI:
675 https://doi.org/10.1111/eva.70086

676 Gao BY, Reynolds DR, Zhai BP, Hu G, Chapman JW, 2020. The 'migratory
677 connectivity' concept, and its applicability to insect migrants. *Move. Ecol.* **8**:48.
678 DOI: https://doi.org/10.1073/pnas.2317646121

679 Gao BY, Wotton KR, Hawkes WLS, Menz MHM, Reynolds DR, Zhai BP, Hu G,
680 Chapman JW, 2020. Adaptive strategies of high-flying migratory hoverflies in
681 response to wind currents. *Proc. R. Soc. B* **287**:20200406. DOI:
682 https://doi.org/10.1098/rspb.2020.0406

683 Gao BY, Reynolds DR, Hu G, Chapman JW, 2024. Effects of nocturnal celestial
684 illumination on high-flying insect migration. *Phil. Trans. Roy. Soc. B*
685 **379**:20230115. DOI: https://doi.org/10.1098/rstb.2023.0115

686 Gao FQ, Chen H, Kyerematen R, Hu G, Early R, Chapman JW, 2025. High migratory
687 potential of fall armyworm in West Africa despite stable temperatures and widely
688 available year-round habitats. *Insect Sci.* https://doi.org/10.1111/1744-
689 7917.13502 .

690 Goergen G, Kumar PL, Sankung SB, Togola A, Tamo M, 2016. First report of
691 outbreaks of the fall armyworm *Spodoptera frugiperda* (J E Smith) (Lepidoptera,
692 Noctuidae), a new alien invasive pest in west and central Africa. *PLoS One*
693 **11**:e0165632. DOI: https://doi.org/10.1371/journal.pone.0165632

694 Goforth KM, Lohmann CMF, Gavin A, Henning R, Harvey A, Hinton TL, Lim DS,
695 Lohmann KJ, 2025. Learned magnetic map cues and two mechanisms of
696 magnetoreception in turtles. *Nature* **638**:1015–1022. DOI:
697 https://doi.org/10.1038/s41586-024-08554-y

698 Grob R, Wegmann JW, Rössler W, Fleischmann PN, 2024. *Cataglyphis* ants have a
699 polarity-sensitive magnetic compass. *Curr. Biol*. **34**:5833-5838. DOI:
700 https://doi.org/10.1016/j.cub.2024.11.012

701 Guo J, Fu X, Zhao S, Shen X, Wyckhuys KAG, Wu K, 2020. Long-term shifts in
702 abundance of (migratory) crop-feeding and beneficial insect species in
703 northeastern Asia. *J. Pest Sci*. **93**:583-594. DOI: https://doi.org/10.1007/s10340-
704 019-01191-9

705 Holland RA, Wikelski M, Wilcove DS. 2006, How and why do insects migrate?
706 *Science*, **313**:794-796. https://doi.org/10.1126/science.1127272

707 Hu G, Lim KS, Horvitz N, Clark SJ, D. R. Reynolds, N. Sapir, J. W. Chapman, Mass
708 seasonal bioflows of high-flying insect migrants. *Science* **354**:1584-1587 (2016).
709 DOI: https://doi.org/10.1126/science.aah4379

710 Hu G, Feng HQ, Otuka A, Reynolds DR, Drake VA, Chapman JW, 2025. The east
711 Asian Insect flyway: geographical and climatic factors driving migration among
712 diverse crop pests. *Annu. Rev. Entomol*. **70**:1-22. DOI: https://doi.org/10.1146/
713 annurev-ento-012524-124018

714 Huang JR, Feng HQ, Drake VA, Reynolds DR, Gao BY, Chen FJ, Zhang GY, Zhu J,
715 Gao YB, Zhai BP, Li GP, Tian CH, Huang B, Hu G, Chapman JW, 2024. Massive
716 seasonal high-altitude migrations of nocturnal insects above the agricultural
717 plains of East China. *Proc. Nat. Acad. Sci. USA*. **121**:e2317646121.
718 DOI: https://doi.org/10.1073/pnas.2317646121

719 Hore PJ, Mouritsen H, 2016. The radical-pair mechanism of magnetoreception.
720 *Annu. Rev. Biophys.* **45**:299-344. DOI: https://doi.org/10.1146/annurev-biophys-
721 032116-094545

722 Jin MH, Liu B, Zheng WG, Liu CH, Liu ZX, He Y, Li XK, Wu C, Wang P, Liu KY, Wu
723 SG, Liu HW, Chakrabarty S, Yuan HB, Wilson K, Wu KM, Fan W, Xiao YT, 2023.
724 Chromosome-level genome of black cutworm provides novel insights into
725 polyphagy and seasonal migration in insects. *BMC Biology* **21**:2. DOI:
726 https://doi.org/10.1186/s12915-022-01504-y

727 Kenis M, Benelli G, Biondi A, Calatayud PA, Day R, Desneux N, Harrison RD,
728 Kriticos D, Rwomushana I, van den Berg J, Verheggen F, Zhang YJ, Agboyi LK,
729 Ahissou RB, Ba MN, Wu KM, 2023. Invasiveness, biology, ecology, and
730 management of the fall armyworm, *Spodoptera frugiperda*. *Entomol. Gen.*
731 **43**:187–241. DOI: https://doi.org/10.1127/entomologia/2022/1659

732 Li XJ, Wu MF, Ma J, Gao BY, Wu QL, Chen AD, Liu J, Jiang YY, Zhai BP, Early R,

Chapman JW, Hu G, 2020. Prediction of migratory routes of the invasive fall armyworm in eastern China using a trajectory analytical approach. *Pest Manag. Sci.* **76**:454-463. DOI: https://doi.org/10.1002/ps.5530

Massy R, Hawkes WLS, Doyle T, Troscianko J, Menz MHM, Roberts NM, Chapman JW, Wotton KR, 2021. Hoverflies use a time-compensated sun compass to orientate during autumn migration. *Proc. R. Soc. B* **288**:20211805. DOI: https://doi.org/10.1098/rspb.2021.1805

Menz MHM, Scacco M, Bürki-Spycher HM, Williams HJ, Reynolds DR, Chapman JW, Wikelski M, 2022. Individual tracking reveals long-distance flight-path control in a nocturnally migrating moth. *Science* **377**:764-768. DOI: https://doi.org/10.1126/science.abn166

Mouritsen H & Frost B, 2002. Virtual migration in tethered flying monarch butterflies reveals their orientation mechanisms. *Proc. Nat. Acad. Sci. USA*. **99**:10162-10166. DOI: https://doi.org/10.1073/pnas.152137299

Mouritsen H, 2018. Long-distance navigation and magnetoreception in migratory animals. *Nature* **558**:50-59. https://doi.org/10.1038/s41586-018-0176-1

Nagoshi RN & Meagher RL, 2008. Review of fall armyworm (Lepidoptera: Noctuidae) genetic complexity and migration. *Fla Entomol* **91**:546-554. DOI: https://doi.org/10.1653/0015-4040-91.4.546

Reppert SM, Guerra PA, Merlin C, 2016. Neurobiology of monarch butterfly migration. *Annu. Rev. Entomol.* **61**:25-42. DOI: https://doi.org/10.1146/annurev-ento-010814-020855

Srygley RB & Dudley R, 2008. Optimal strategies for insects migrating in the flight boundary layer: Mechanisms and consequences. *Integr. Comp. Biol.* **48**:119-133. DOI: https://doi.org/10.1093/icb/icn011

Tay WT, Meagher RL, Czepak C, Groot AT, 2023. *Spodoptera frugiperda*: Ecology, evolution, and management options of an invasive species. *Annu. Rev. Entomol.* **68**:299-317. DOI: https://doi.org/10.1146/annurev-ento-120220-102548

Tong DD, Zhang L, Wu NN, Xie DJ, Fang GJ, Coates BS, Sappington TW, Liu YQ, Cheng YX, Xia JX, Jiang XF, Zhan SA, 2022. The oriental armyworm genome yields insights into the long-distance migration of noctuid moths. *Cell Rep.* **41**:111843. DOI: https://doi.org/10.1016/j.celrep.2022.111843

Wan GJ, Hayden AN, Iiams SE, Merlin C, 2021. Cryptochrome 1 mediates light-dependent inclination magnetosensing in monarch butterflies. *Nat. Comm.* **12**:771. DOI: https://doi.org/10.1038/s41467-021-21002-z

Warrant EJ. & Dacke M. 2011. Vision and visual navigation in nocturnal insects. *Ann. Rev. Entomol.* **56**:239-254. DOI: https://doi.org/10.1146/annurev-ento-120709-144852

Warrant EJ, Frost B, Green K, Mouritsen H, Dreyer D, Adden A, Brauburger K, Heinze S, 2016. The Australian Bogong moth *Agrotis infusa*: A long-distance nocturnal navigator. *Front. Behav. Neurosci.* **10**:77. DOI: https://doi.org/10.3389/fnbeh.2016.00077

Werber Y, Adin E, Chapman JW, Reynolds DR, Sapir N, 2025. Active navigation and meteorological selectivity drive mass intercontinental insect migration patterns through the Levant. *Proc. R. Soc. B* **292**:20250587. DOI: https://doi.org/10.1098/rspb.2025.0587

Westbrook J, Fleischer S, Jairam S, Meagher R, Nagoshi R, 2019. Multigenerational migration of fall armyworm, a pest insect. *Ecosphere* **10**:e02919. DOI: https://doi.org/10.1002/ecs2.2919

Wu QL, Jiang YY, Liu J, Hu G, Wu KM, 2021. Trajectory modeling revealed a southwest-northeast migration corridor for fall armyworm *Spodoptera frugiperda* (Lepidoptera: Noctuidae) emerging from the North China Plain. *Insect Sci*. **28**:649-661. DOI: https://doi.org/10.1111/1744-7917.12852

Wu MF, Qi GJ, Chen H, Ma J, Liu J, Jiang YY, Lee GS, Otuka A, Hu G, 2022. Overseas immigration of fall armyworm, *Spodoptera frugiperda* (Lepidoptera: Noctuidae) invading Korea and Japan in 2019. *Insect Sci.* **29**:505-520. DOI: https://doi.org/10.1111/1744-7917.12940

Satterfield DA, Sillett TS, Chapman JW, Altizer S, Marra PP, 2020. Seasonal insect migrations: massive, influential, and overlooked. *Front. Ecol. Environ.* **18**:335-344. DOI: https://doi.org/10.1002/fee.2217

Sun XX, Hu CX, Jia HR, Wu QL, Shen XJ, Zhao SY, Jiang YY, Wu KM, 2021. Case study on the first immigration of fall armyworm, *Spodoptera frugiperda* invading into China. *J. Integr. Agri.* **20**:664-672. DOI: https://doi.org/10.1016/s2095-3119(19)62839-x

Xu JJ, Pan W, Zhang YC, Li Y, Wan GJ, Chen FJ, Sword GA, Pan WD, 2017. Behavioral evidence for a magnetic sense in the oriental armyworm, *Mythimna separata*. *Biol. Open* **6**:340-347. DOI: https://doi.org/10.1242/bio.022954

Xu JJ, Jarocha LE, Zollitsch T, Konowalczyk M, Henbest KB, Richert S, Golesworthy MJ, Schmidt J, Déjean V, Sowood DJC, Bassetto M, Luo J, Walton JR, Fleming J, Wei Y, T, Pitcher TL, Moise G, Herrmann M, Yin H, Wu HJ, Bartölke R, Käsehagen SJ, Horst S, Dautaj G, Murton PDF, Gehrckens AS, Chelliah Y, Takahashi JS, Koch KW, Weber S, Solov'yov IA, Xie C, Mackenzie SR, Timmel CR, Mouritsen H, Hore PJ, 2021. Magnetic sensitivity of cryptochrome 4 from a migratory songbird. *Nature* **594**:535-540. DOI: https://doi.org/10.1101/2024.09.19.613835

Supplementary information

Table S1. Detailed data of flight orientation behavior assay.

Group	Period	MV	*R**	n	*P*
Fall Exp. Field	I	183.6	1.76	29	$P < 0.001$
	II	191.0	1.16	29	$0.01 < P < 0.025$
	III	158.1	0.34	29	$0.5 < P < 0.9$
	IV	354.3	1.49	29	$0.001 < P < 0.005$
	V	167.7	1.62	29	$P < 0.001$
Spring Exp. Field	I	347.4	1.59	28	$P < 0.001$
	II	319.1	1.39	28	$0.001 < P < 0.005$
	III	293.7	0.67	28	$0.1 < P < 0.5$
	IV	245.2	0.95	28	$0.05 < P < 0.1$
	V	343.8	1.84	28	$P < 0.001$
Fall Exp. Lab	I	182.9	1.77	27	$P < 0.001$
	II	184.9	1.31	27	$0.005 < P < 0.01$
	III	111.3	0.69	27	$0.1 < P < 0.5$
	IV	4.1	2.17	27	$P < 0.001$
	V	137.6	1.04	27	$0.025 < P < 0.05$
Fall Control	I	180.3	2.10	26	$P < 0.001$
	II	184.1	1.94	26	$P < 0.001$
	III	195.2	1.43	26	$0.001 < P < 0.005$
	IV	6.1	1.63	26	$P < 0.001$
	V	183.0	1.81	26	$P < 0.001$
Fall Exp. Dark	I	218.48	1.50	31	$0.001 < P < 0.005$
	II	41.03	0.55	31	$0.1 < P < 0.5$
Fall Exp. BMVC	I	114.51	0.32	30	$0.5 < P < 0.9$
	II	215.76	0.65	30	$0.1 < P < 0.5$
	III	105.72	0.31	30	$0.5 < P < 0.9$
	IV	191.21	0.66	30	$0.1 < P < 0.5$

Table S2. Multiple comparison results of the mean Rayleigh's *r* values of Exp. Spring across different experimental phases, using the Wilcoxon rank-sum test with multiple comparison correction performed by the Benjamini-Hochberg method.

Experiment	Comparison group	*W* value	*P* value	Median difference
Spring Exp. Field	IV – V	307	0.334	-0.072
	III-V	305	0.334	-0.160
	II-V	279	0.280	-0.175
	I-V	200	0.014	-0.260
	III-IV	384	0.903	-0.088
	II-IV	354	0.676	-0.103
	I-IV	286	0.28	-0.189
	II-III	360	0.676	-0.015
	I-III	316	0.363	-0.100
	I-II	337	0.536	-0.086
Fall Exp. Field	IV-V	434	0.961	0.047
	III-V	404	0.961	0.005
	II-V	432	0.961	-0.024
	I-V	467	0.961	0.010
	III-IV	381	0.961	-0.042
	II-IV	421	1.000	-0.071
	I-IV	442	0.961	-0.037
	II-III	447	0.961	-0.029
	I-III	478	0.961	0.005
	I-II	465	0.961	0.034
Fall Exp. Lab	IV-V	369	0.945	0.255
	III-V	339	0.835	0.168
	II-V	395	0.835	0.232
	I-V	446	0.693	0.316
	III-IV	331	0.835	-0.087
	II-IV	382	0.857	-0.023
	I-IV	416	0.762	0.061

	II-III	417	0.762	0.064
	I-III	482	0.423	0.148
	I-II	438	0.693	0.084
Fall Control	IV-V	347	0.949	-0.053
	III-V	328	0.949	-0.129
	II-V	342	0.949	-0.022
	I-V	378	0.949	-0.028
	III-IV	330	0.949	-0.076
	II-IV	352	0.949	0.031
	I-IV	383	0.949	0.025
	II-III	374	0.949	0.107
	I-III	398	0.949	0.101
	I-II	374	0.949	-0.007

Table S3. Multiple comparisons of mean Rayleigh test *r* values across experimental conditions using the Wilcoxon rank-sum test (adjusted by the Benjamini-Hochberg method).

Comparison group	*W* value	*P* value	Median difference
B-A	9084	0.320	-0.134
C-A	7632	0.012	-0.190
D-A	2407	0.537	0.029
E-A	3252	0.0002	0.165
F-A	13740	< 0.0001	0.224
C-B	7934	0.222	-0.056
D-B	2386	0.260	0.163
E-B	2958	0.0007	0.298
F-B	12544	< 0.0001	0.358
D-C	2543	0.036	0.219
E-C	3186	< 0.0001	0.354
F-C	13174	< 0.0001	0.414
E-D	666	0.014	0.136
F-D	2791	< 0.0001	0.195
F-E	2286	0.068	0.059

Note: A: Fall Exp. Field; B: Fall Exp. Lab; C: Fall Control; D: Fall Exp. Dark I; E: Fall Exp. Dark II; F: Fall Exp. BMVC.

Table S4. Tukey test for mean angular velocity (directional change per second) across experimental conditions.

Comparison group	Difference	Confidence Interval (95%)	*P* value
B-A	-2.42	-7.76 – 2.92	0.79
C-A	-4.27	-9.66 – 1.12	0.21
D-A	-1.84	-10.67 – 7.00	0.99
E-A	10.46	1.62 – 19.29	0.01
F-A	13.49	7.98 – 19.00	< 0.001
C-B	-1.85	-7.33 – 3.64	0.93
D-B	0.59	-8.3 – 9.48	1.00
E-B	12.88	3.99 – 21.77	< 0.001
F-B	15.92	10.32 – 21.52	< 0.001
D-C	2.43	-6.49 – 11.36	0.97
E-C	14.72	5.80 – 23.65	< 0.001
F-C	17.76	12.11 – 23.41	< 0.001
E-D	12.29	0.95 – 23.63	0.02
F-D	15.33	6.33 – 24.32	< 0.001
F-E	3.04	-5.96 – 12.03	0.93

Note: A: Fall Exp. Field; B: Fall Exp. Lab; C: Fall Control; D: Fall Exp. Dark-I; E: Fall Exp. Dark-II; F: Fall Exp. BMVC.

829 **Table S5. Multiple comparisons of mean Rayleigh test *r* values across**

830 **experimental conditions using the Wilcoxon rank-sum test adjusted by the**

831 **Benjamini-Hochberg method.**

Comparison group	*W* value	*P* value	Median difference
B-A	666	0.026	0.1355
C-A	676	0.008	0.1534
D-A	711	0.002	0.2041
E-A	718	0.002	0.2184
F-A	686	0.006	0.1913
C-B	523	0.512	0.0179
D-B	583	0.169	0.0686
E-B	623	0.056	0.0829
F-B	557	0.313	0.0557
D-C	529	0.372	0.0507
E-C	576	0.135	0.065
F-C	490	0.602	0.0378
E-D	490	0.602	0.0143
F-D	429	0.764	-0.0129
F-E	378	0.4	-0.0271

832 **Note:** A: Fall Exp. Dark-I; B: Fall Exp. Dark-II; C: Fall Exp. BMVC-I; D: Fall Exp.

833 BMVC-II; E: Fall Exp. BMVC-III; F: Fall Exp. BMVC-IV.

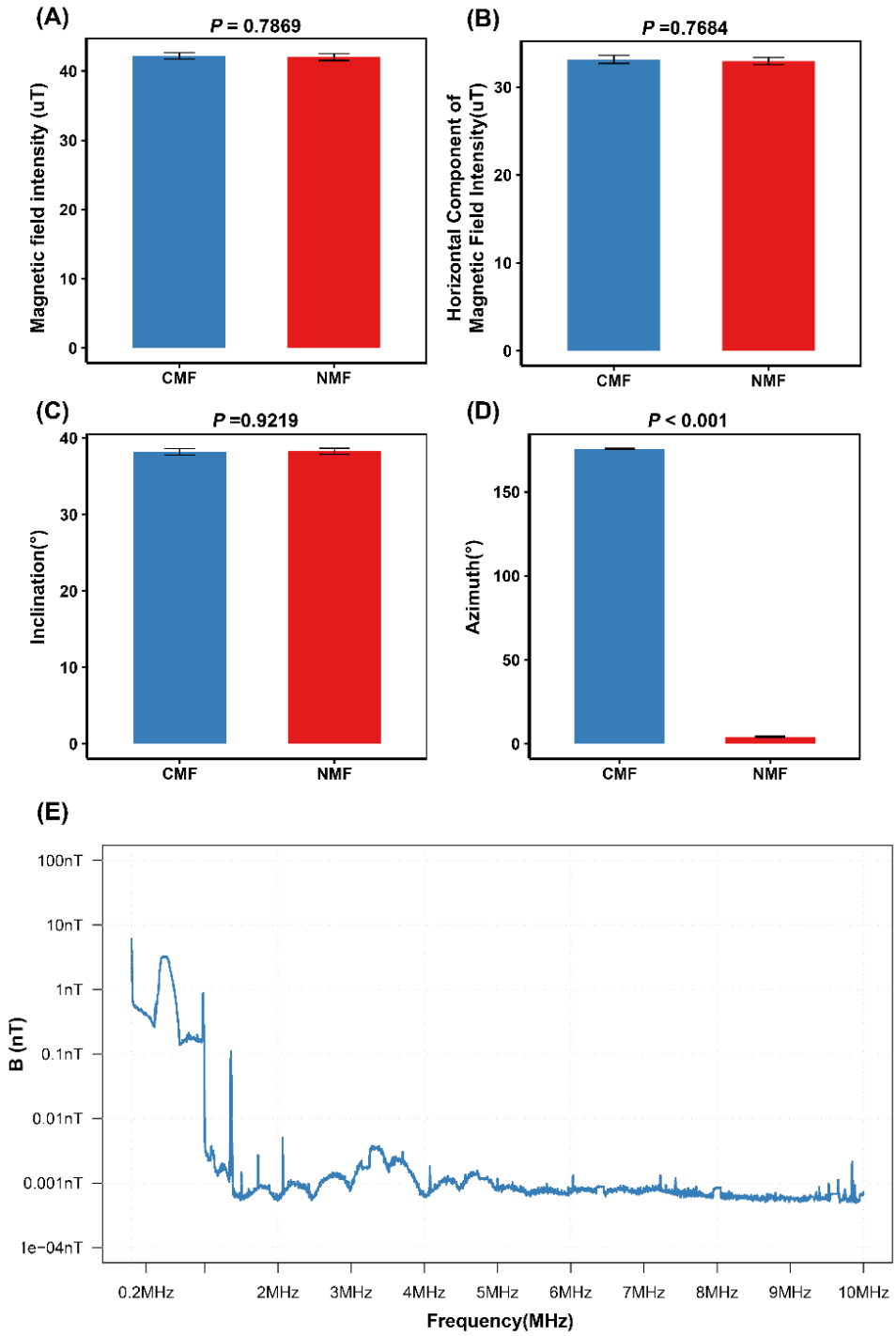

Fig. S1. The magnetic field conditions during experimental procedures in 2023 and 2024. A Comparison of total magnetic field strength between the controlled magnetic field (CMF) and normal magnetic field (NMF) (*t*-test, E_{CMF} = 42.21 μT, E_{NMF} = 42.02 μT, *P* = 0.79), showing no significant difference. **B** There is no significant difference in the intensity of the horizontal component between CMF and NMF (*t*-test, H_{CMF} = 31.18, H_{NMF} = 31.35, *P* = 0.813). **C** There is no significant difference in magnetic inclination between CMF and NMF (*t*-test, α_{CMF} = 38.22°, α_{NMF} = 38.28°, *P* =

0.92). **D** Comparison of magnetic azimuth between CMF and NMF, demonstrating a highly significant difference (*t*-test, β_{CMF} =175.62°, β_{NMF} = 4.11°, $P < 0.001$). **E** The magnetic component *B*, measured in nanoteslas (nT), of the time-dependent electromagnetic field across a 10 kHz resolution bandwidth (RBW), was analyzed as a function of frequency f, expressed in megahertz (MHz). The data shown in the figure represents the maximum locked values observed over a 40-minute period at the experimental location (23.604°N, 101.977°E). Measurements were conducted using the NF5035 spectrum analyzer, MDF9400 magnetic field antenna, MDF960X preamplifier (with a gain of 25 dB), and a 10-meter Anoni RF cable. The spectrum in the frequency range of 1 MHz to 10 MHz was first measured using the antenna paired with the preamplifier. Subsequently, low-frequency noise within the range of 2 kHz to 1 MHz was detected using the internal probe of the spectrum analyzer. In the low-frequency range, significant peaks are observed, particularly in the0.2-1 MHz region, where the magnetic field intensity is notably higher. In contrast, within the frequency range of 1 MHz to 10 MHz, the noise intensity is relatively low, ranging between 0.01 nT and 0.001 nT. The overall trend in this range is fairly stable, with only minor fluctuations at specific frequency points.

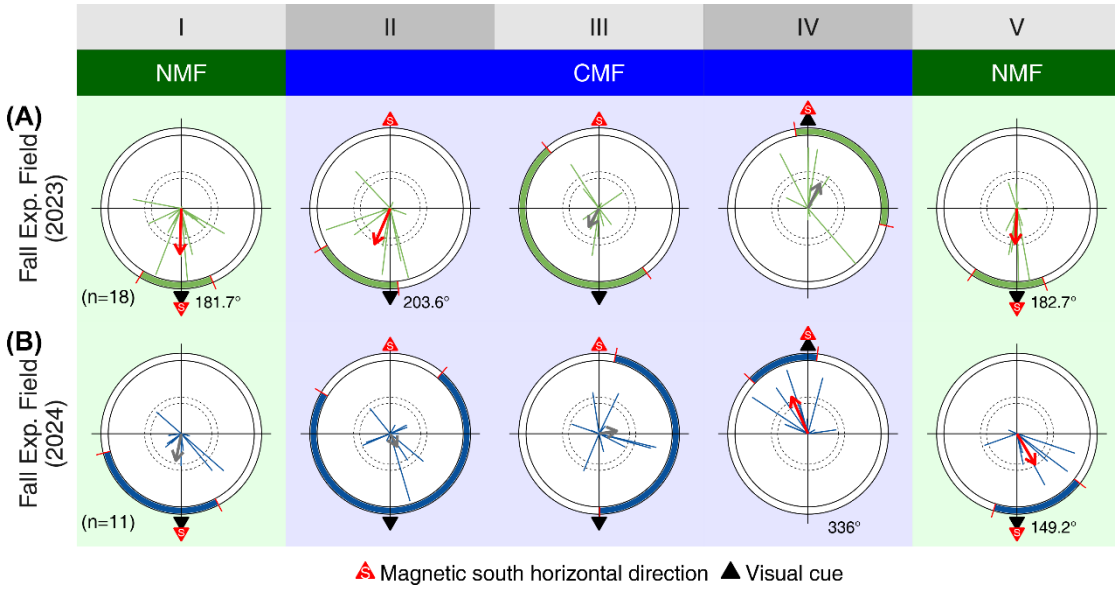

Fig. S2 Year-specific analysis of orientation behavior in fall field-captured fall armyworms (2023 and 2024). A Orientation behavior of the field-captured population in fall 2023. **B** Orientation behavior of the field-captured population in fall 2024. Experiments were conducted using fall armyworms captured from the field, revealing consistent orientation behavior across both years. In both 2023 and 2024, moths oriented significantly toward the visual cue when visual and geomagnetic cues were aligned. However, after reversing the magnetic field, the strength of directional orientation gradually diminished. Due to limited sample sizes in each year, data from both years were pooled for a comprehensive analysis, as presented in Fig. 2B.

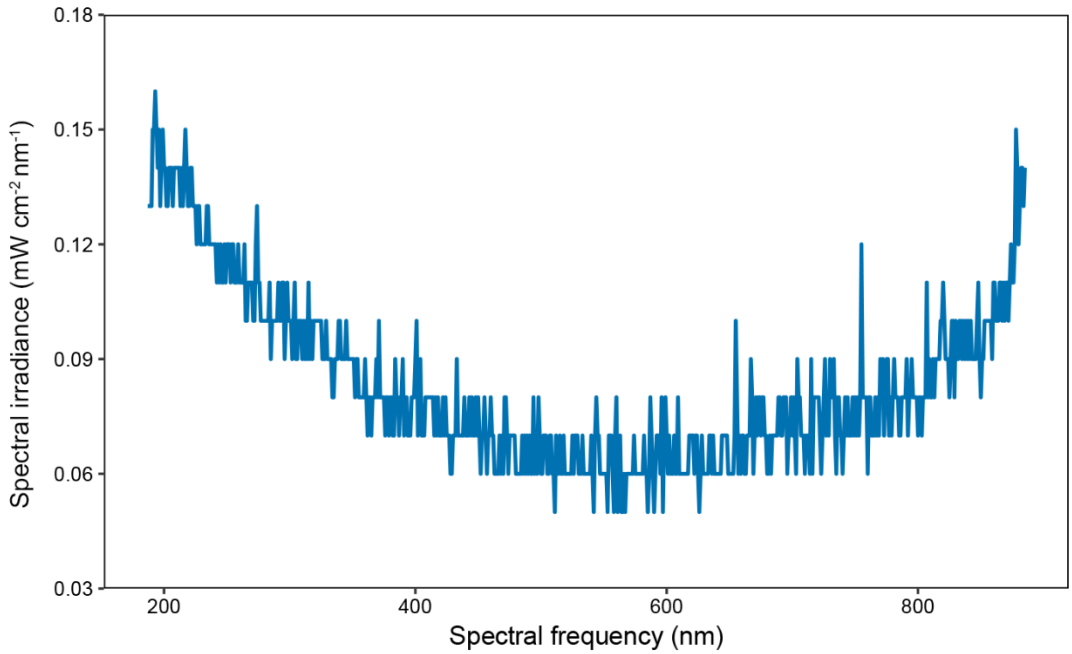

Fig. S3. Spectral distribution of light provided by the full-spectrum lamp. The spectral distribution of the full-spectrum lamp used in the experiment was measured using an ATP2000P spectrometer (Optosky Technology Co. Ltd., Xiamen, China). The sensor was positioned vertically upward at the location originally occupied by the moth to measure the spectral irradiance of the light after it passed through the softbox, diffusion paper, and transparent acrylic cover. The results indicate that light radiation was detectable across most wavelengths between 200 nm and 850 nm, confirming that: The experimental system provides a full-spectrum light environment spanning ultraviolet (UV) to near-infrared (NIR) wavelengths, covering the visual range relevant to moths. And the acrylic plate and diffusion paper did not significantly block light radiation at any specific wavelength, ensuring uniform spectral exposure within the flight arena. The ambient light level in the experimental environment was measured to be below 1 lux using a Testo 540 lux meter, manufactured by Testo SE & Co. KGaA (Titisee-Neustadt, Germany).

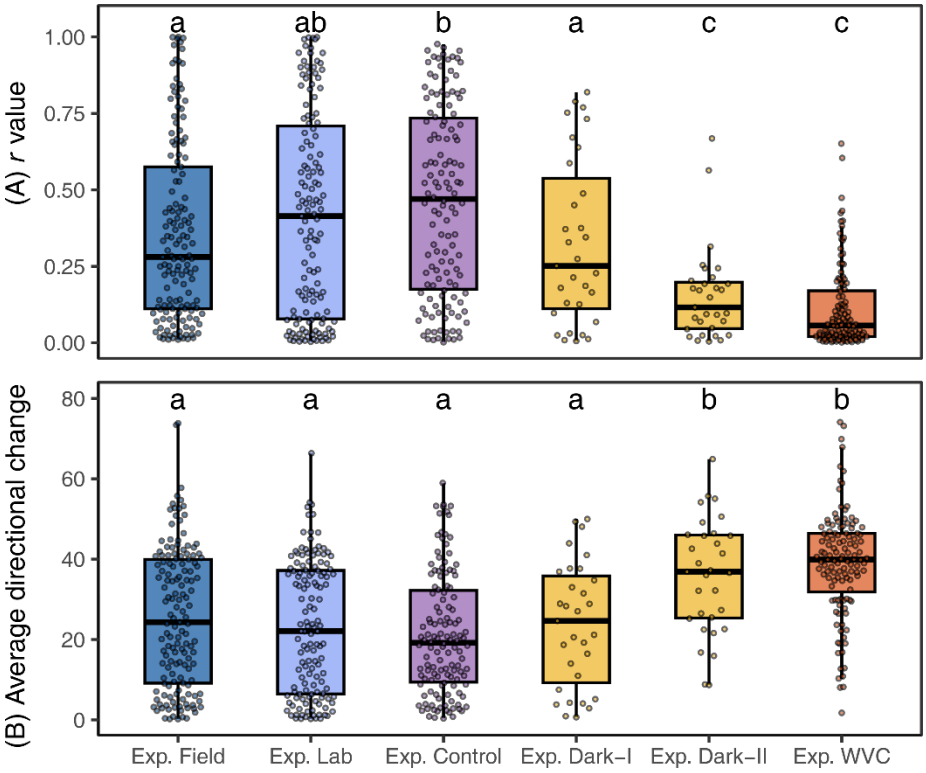

Fig. S4 The lack of visual cues and other necessary visual information significantly affects moth orientation ability and flight stability. A Box plots show the distribution of Rayleigh test *r* values for individual orientations of moths in different treatment groups. **B** Box plots show the distribution of average directional degree change per second, reflecting flight stability, across treatment groups. Boxes represent the interquartile range (IQR), with the horizontal line inside indicating the median. The "whiskers" extend to the most extreme data points within 1.5 times the IQR. Error bars indicate data variability, facilitating comparison between groups. Pairwise comparisons in **A** were conducted using the Mann-Whitney *U* test with multiple comparisons corrected by the Benjamini-Hochberg method. Detailed statistical results are provided in Supplementary Table S3. In **B**, comparisons were performed using one-way ANOVA followed by Tukey's HSD post hoc test. Groups labeled with different letters differ significantly ($P < 0.05$). Detailed statistical results are provided in Supplementary Table S4.